Chapter III-2 Geometric modelling of linear CCDs and panoramic imagers

K. Jacobsen
Leibniz University Hannover, Germany

ABSTRACT: With only a few exceptions, optical spaceborne cameras are CCD-line cameras. The different orientation methods such as the mathematical correct geometric reconstruction, the sensor oriented, bias corrected rational polynomial coefficients (RPCs) and the approximate solutions such as 3-D affine transformation, direct linear transformation and terrain dependent RPCs are described with their potential, problems and required number and distribution of control points. Aerial CCD-line scanner systems today are in use as three-line scanners, usually supported by GPS and inertial measurement units (IMU). The aerial triangulation of three line scanners, required for reliable and more precise results, is discussed. Panoramic imagers have been used in space by the CORONA and the KVR1000 systems. Their high resolution images are still important today. In addition, aerial panoramic imagers are in use mainly for military applications. The geometric handling of panoramic images by transformation to perspective geometry and the determination of the platform motion influence by self calibration with special additional parameters is explained.

KEY WORDS: Image geometry, orientation, self calibration, optical satellite images, aerial CCD-line scanner images, panoramic cameras

1 SPACEBORNE SYSTEMS

1.1 Introduction

Very high resolution optical space images like those from IKONOS, QuickBird, OrbView-3, Cartosat-2, Kompsat-2, Resource DK1, EROS B and WorldView-1 today compete with classical aerial images. The information content of the space images can be compared with aerial photos having a scale up to 1:25,000, but the geometric conditions should also be on a similar level, requiring satisfactory mathematical handling. Images close to the original, initially named as level 1A, and images projected to a specified object surface, originally named as level 1B, and even epipolar images are available. The geometric handling has to respect the given image product.

1.2 Geometry of combined CCD-lines

Spaceborne CCD-line sensors are usually based on a combination of individual CCD-lines merged together, based on a combination of sub-images, corrected by sensor calibration (Fig. 1) (Jacobsen 1997). These merged images are still named original images, because the real original images are not available to the user.
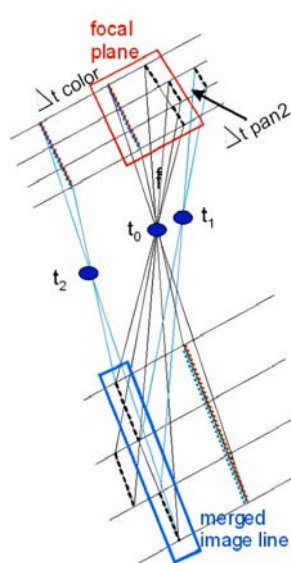

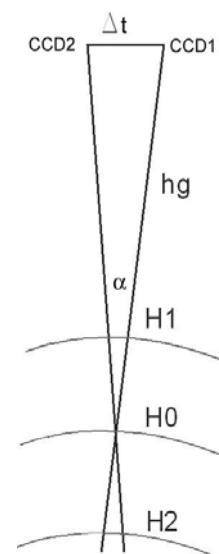Figure 1. Combination of CCD-sensors to a homogenous virtual CCD-line.

Figure 2. Mismatch of CCD-lines as a function of height and reference height.

The merged images in theory are only correct for the reference height H0 (Fig. 2); for another height such as H1 or H2, a mismatch of neighbouring sub-scenes occurs. For instance, for IRS-1C and IRS-1D, a mismatch of 1 pixel appears for height differences of 450 m against the reference height H0 and for QuickBird a 1 pixel mismatch will appear at a height difference of 2.8 km; that means it is never important.

1.3 *Image geometry and image products*

The classical optical satellites have a fixed orientation in relation to the satellite orbit during imaging. Today the imaging satellites are equipped with reaction wheels or control moment gyros, allowing a permanent, fast and precise change of the view direction. So usually the images are not taken in the orbit direction just based on the movement of the satellite: they are scanned directly in relation to the specified ground window. This may be in a north-south direction, but for stereo imaging it is often also in an east-west direction. IKONOS is equipped with a second CCD-line, allowing also the scan with the TDI-sensor against the movement in the orbit; that means from south to north. Not all satellites are able to generate a sufficient image quality because of the speed of the satellite in the orbit; they are extending the imaging time by asynchronous or slow down mode (Fig. 3). So the sampling rate of QuickBird is limited to 6900 lines/sec, with the 0.61 m ground sampling distance (GSD). This would correspond to 4.2 km/sec orbit speed, but the satellite has a foot print speed of 7.1 km/sec, requiring a slow down factor of 1.7. OrbView-3 and EROS have to use the asynchronous mode also to obtain sufficient image quality. This asynchronous mode has to be respected by the orientation procedure.

For IKONOS, only images projected to a surface with constant height are distributed as Geo-images (Fig. 4). There is still confusion with the product names – the expression level 1B is used for QuickBird Basic Imagery (original images) while the expression level 1B traditionally is used for projected images. For QuickBird, in addition to the original images (Basic Imagery) and the images projected to a surface with constant height (OrthoReady Standard), images are also projected to the rough DEM GTOPO30 (Standard Imagery) for distribution. For OrbView-3, at first only the original images (OrbView Basic) could be ordered but now projected images are also available as OrbView Geo.
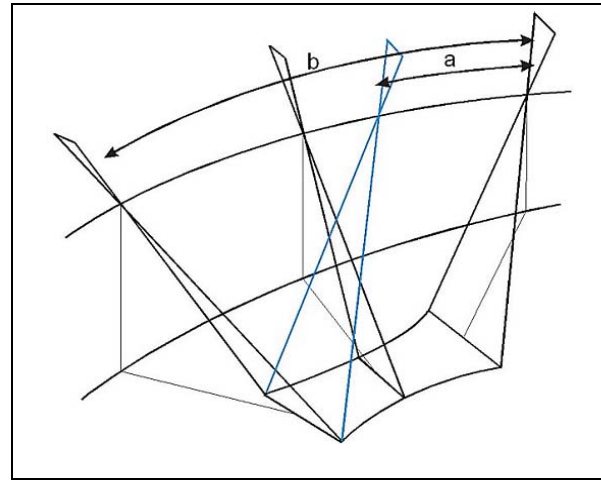

Figure 3. Asynchronous image mode (slow down mode) by permanent change of view direction during imaging - extension of imaging time. Slow down factor = b/a.
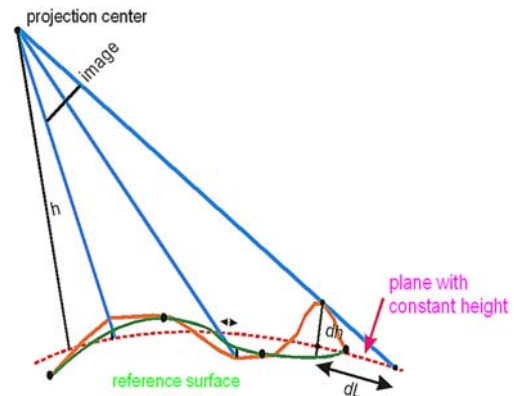

Figure 4. Image products.
1. Image = original image (level 1A-type) e.g. QuickBird Basic, OrbView Basic.
2. Projection to plane with constant height (level 1B-type) e.g. IKONOS Geo, QuickBird OR Standard.
3. Swinging line = QuickBird Standard – related to the rough DEM GTOPO30.

1.4 *Orientation of CCD-line images.*

1.4.1 *Sensor oriented RPCs*
Sensor oriented Rational Polynomial Coefficients (RPCs) from the satellite image vendors are describing the location of image positions as a function of the object coordinates (longitude, latitude, height) by the ratio of polynomials (Grodecki 2001). The sensor related RPCs are based on the direct sensor orientation of the satellite together with information about the inner orientation and have an accuracy depending upon the quality of the direct sensor information. Third order polynomials with 20 coefficients are used, so with 80 coefficients the relation of the image coordinates to the object coordinates can be described (Formula 1).

Based on the sensor oriented RPCs, a terrain relief correction can be made; that means the value dL in Figure 4 together with the direction of this vector are computed. This can be made for level 1A-

and level 1B-type images. The resulting object positions can be related to ground control points by two-dimensional transformation leading to the bias corrected RPC solution. For IKONOS, a simple shift of the terrain relief corrected scene to control points is usually sufficient; for other sensors, or old IKONOS images without the information of the reference height, a two-dimensional affinity transformation of the computed object coordinates to the control points is required.

$$xij = \frac{Pi1(X,Y,Z)j}{Pi2(X,Y,Z)j} \qquad yij = \frac{Pi3(X,Y,Z)j}{Pi4(X,Y,Z)j}$$

$Pn(X,Y,Z)j = a_1 + a_2*Y + a_3*X + a_4*Z + a_5*Y*X + a_6*Y*Z + a_7*X*Z + a_8*Y^2 + a_9*X^2 + a_{10}*Z^2 + a_{11}*Y*X*Z + a_{12}*Y^3 + a_{13}*Y*X^2 + a_{14}*Y*Z^2 + a_{15}*Y^2*X + a_{16}*X^3 + a_{17}*X*Z^2 + a_{18}*Y^2*Z + a_{19}*X^2*Z + a_{20}*Z^3$

Formula 1. Rational polynomial coefficients.
  xij, yij = normalized scene coordinates
  X,Y   = normalized geographic object coordinates
  Z   = height

1.4.2 *Terrain dependent RPCs*
The relation of the scene to object coordinates can be approximated by RPCs also just based on control points. Of course, it is not possible to determine 80 orientation unknowns – this would require at least 40 ground control points per scene, so only the most important RPCs are computed. The number of chosen unknowns is quite dependent upon the number and three-dimensional distribution of the control points. This method cannot be controlled just by the residuals at the control points. Some commercial programs offering this method do not use any statistical checks for high correlation of the unknowns, making the correct handling very dangerous. A test with a commercial program using this method was leading with IKONOS data to control point residuals below 1 m and did not mark any problems. Even in an area within the range of the control points, discrepancies in the range of 50 m appeared at check points and outside the range of the control points, discrepancies exceeding 500 m. This method cannot be controlled; it has to be avoided and it is absolutely not a serious solution. In general, available orientation information should be used to reduce the required number and distribution of control points.

1.4.3 *Three-dimensional affine transformation*
Like the terrain dependent RPCs, the three-dimensional affine transformation is not using any available sensor orientation information. The 8 unknowns for the transformation of the object point

coordinates to the image coordinates have to be computed based on control points located not in the same plane (Formula 2) (Hanley et al. 2002). At least 4 well distributed control points are required. The 3-D affinity transformation is based on a parallel projection, which is approximately given in the orbit direction but not in the direction of the CCD-line.

$$xij = a1 + a2*X + a3*Y + a4*Z$$
$$yij = a5 + a6*X + a7*Y + a8*Z$$

Formula 2. 3-D affine transformation.

The not precise mathematical model of parallel projection is not a problem for a narrow field of view if in addition the height differences in the object space are not very large. For large height differences and unknown slow down mode, extended formulae are introduced by Jacobsen (2007b). Formula 3 respects the perspective geometry in the CCD-line direction and also a possible asynchronous imaging mode.

$$xij = a1 + a2*X + a3*Y + a4*Z + a9*X*Z + a10*Y*Z$$
$$yij = a5 + a6*X + a7*Y + a8*Z + a11*X*Z + a12*Y*Z$$

Formula 3. Extended 3-D affine transformation.

For the handling of original images, a further extension has been made (Formula 4), which respects that the scene limits projected to the ground may not be parallel to each other.

$$xij = a1 + a2*X + a3*Y + a4*Z + a9*X*Z + a10*Y*Z + a13*X*X$$
$$yij = a5 + a6*X + a7*Y + a8*Z + a11*X*Z + a12*Y*Z + a14*X*Y$$

Formula 4. Extended 3-D affine transformation for original images.

1.4.4 *Direct Linear Transformation (DLT)*
Like the 3-D affine transformation, the DLT is not using any pre-information about image orientation. The 11 unknowns for the transformation of the object coordinates to the image coordinates (Formula 5) have to be determined with at least 6 control points. The small field of view for high resolution satellite images, together with the limited object height distribution in relation to the satellite flying height, is causing more problems with correlation of unknowns as in the 3-D affine transformation. The DLT is based on a perspective image geometry that is available only in the direction of the CCD-line. There is no justification for the use of this method for the orientation of

satellite images having more unknowns than required by other solutions.

$$xij = \frac{L1*X + L2*Y + L3*Z + L4}{L9*X + L10*Y + L11*Z + 1}$$

$$yij = \frac{L5*X + L6*Y + L7*Z + L8}{L9*X + L10*Y + L11*Z + 1}$$

Formula 5. DLT transformation.

1.4.5 *Reconstruction of imaging geometry*

A mathematically correct method of scene orientation is the reconstruction of the imaging geometry. For level 1B-type images, for the geo-referenced scene centre or the first line, the direction to the satellite is available in the image header data. This direction can be intersected with the orbit of the satellite published with its Keppler elements. Depending upon the location of an image point, the location of the corresponding projection centre in the satellite orbit and the view direction can be computed, respecting the Earth rotation and the slow down factor of asynchronous imaging. So the view direction from any ground point to the corresponding projection centre can be reconstructed. This method requires the same number of control points as the sensor oriented RPC-solution; that means it can be used also without control points if the direct sensor orientation is accepted as accurate enough. Otherwise it requires the same two-dimensional transformation of the terrain relief corrected object points to the control points as the sensor oriented RPCs. A slightly different geometric model has been developed by Toutin (Toutin 2003).

In general, similar orientation methods as used for the level 1-B type images can be used for the orientation of original images (level 1A-type), but the handling of original images is more difficult – they are not corrected for effects of high frequency satellite rotations. The level 1B-type images are geo-coded and only need a terrain relief correction and a 2-D improvement of the location, which is close to a datum problem. For this reason, the basic conditions for the approximate solutions are more difficult for original images.

The scene orientation of original space images by geometric reconstruction is not new. At first it had been developed for SPOT images. For instance in Jacobsen (1997), the image geometry is reconstructed based on the given view direction, the general satellite orbit and a few control points. Based on control points, the attitudes and the satellite height are improved. The X- and Y-locations of the projection line are fixed because they are nearly numerically dependent upon the view

direction. In addition, two additional parameters are required for image affinity and angular affinity. The affinity may be caused by incorrect information about flying height, while the angular affinity may be caused by an imprecise perpendicular orientation of the CCD-line to the orbit. Three control points are necessary for these six unknowns. Additional parameters can be introduced if geometric problems exist. Only for scenes with totally unknown orientation will the full sensor orientation with 6 orientation elements be adjusted together with the necessary additional parameters. This requires a good vertical distribution of control points; for flat areas the full orientation cannot be computed. Other solutions use the given sensor orientation together with some required correction parameters. In general, more control points with a good three-dimensional distribution are required if the existing sensor orientation information is not to be used and the view direction is computed by means of control points. The orientation of the original images also can be made with sensor oriented RPCs in an iterative manner. It has to be improved by means of control points, corresponding to the bias corrected RPC solution (Grodecki 2001).

1.4.6 *Comparison of results*

The different orientation methods have been compared with different types of satellite images. As typical examples the results achieved in the Zonguldak test area are shown (Jacobsen 2007c). Zonguldak is located in Turkey at the Black Sea. The control points of the mountainous area range from sea level up to 440 m, so optimal conditions for the approximate orientation solutions exist.
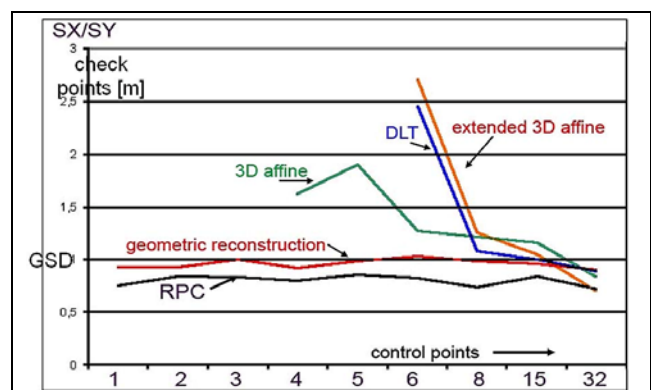

Figure 5. Orientation of IKONOS images, Zonguldak (mountainous), 1.0 m GSD root mean square discrepancies at independent check points as a function of number of control points used.

The bias corrected RPC solution leads even with just one control point to a root mean square error of the independent check points of 0.75 m, corresponding to 0.75 GSD. More control points do not improve the result. With only one control point,

the bias correction is limited to a simple shift. This result has been confirmed by several IKONOS orientations. The geometric reconstruction leads to 0.9 m up to 1.0 m root mean square errors of the check point coordinate components and is also nearly independent of the control point number. An orientation with terrain dependent RPCs could not be accepted because of poor accuracy in areas not directly neighboured to the control points. The 3-D affine transformation requires at least four control points and is not reaching the same accuracy level. Here a higher number of control points improves the result. For the DLT and the extended 3D affine solution, at least six control points are required and only the result with 15 control points is close to the level of the geometric reconstruction and the bias corrected, sensor oriented RPC solution.
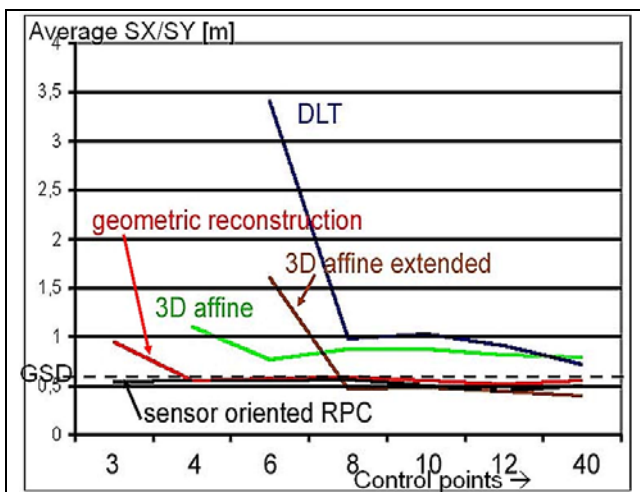

Figure 6. Orientation of QuickBird, Zonguldak, 0.62 m GSD, root mean square discrepancies at independent check points as a function of control point number.
Exception: 40 GCPs = discrepancies at control points.

The orientation of a QuickBird scene in the same area leads to similar results, with the exception that a two-dimensional affine transformation is required after the terrain relief correction, so at least 3 control points are necessary for the orientation of a QuickBird scene. The geometric reconstruction and the bias corrected RPC-solution is on the same level of approximately 0.9 GSD root mean square errors of independent check points. Even with a high number of control points, the 3-D affine transformation does not reach the same accuracy level. This can be explained by the larger field of view of QuickBird and the asynchronous imaging mode. Only with the extended 3-D affine transformation (Formula 3) with at least eight control points is the orientation on the same accuracy level as the mathematical correct solutions.
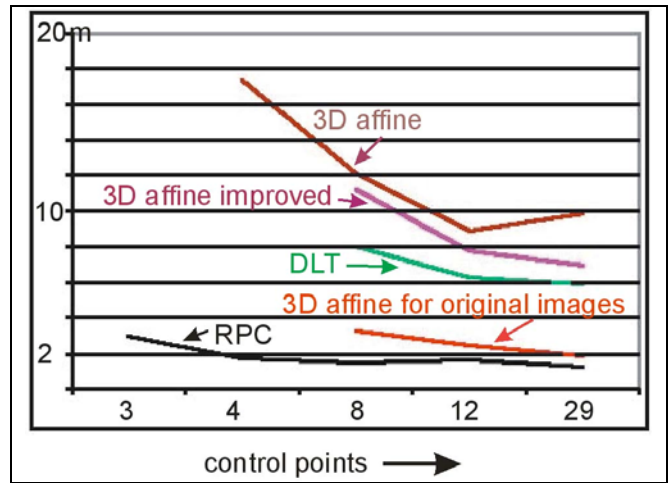

Figure 7. Orientation of OrbView-3 Basic, Zonguldak – root mean square differences at independent check points (vertical direction), depending upon number of control points used.

With OrbView-3 images no accuracy on the GSD-level can be reached as in the shown example (Fig. 7). OrbView-3 has a projected pixel size of 2 m, but with 50% over-sampling 1 m GSD. This may be the reason for just reaching approximately 1.6 GSD accuracy at independent check points. The results achieved with the approximate orientation methods are much larger than the bias corrected, sensor oriented RPC-solution. Only with the 3-D affine transformation for original images (Formula 4) can root mean square differences of 3 up to 2 GSD be reached with at least eight control points.

Table 1. Root mean square differences of independent check points (RMSX / RMSY) based on scene orientation with geometric reconstruction or bias corrected RPC solution.

	level type	GSD [m]	RMSX RMSY [GSD]
ASTER, Zonguldak	A	15	0.7
KOMPSAT-1, Zonguldak	A	6.6	1.3
SPOT, Hannover	A	10	0.5
SPOT 5, Zonguldak	A	5	1.0
SPOT 5, Zonguldak	B	5	1.0
SPOT HRS, Bavaria	A	5 x 10	0.7/1.1
IRS-1C, Hannover	A	5.7	0.9
IRS-1C, Zonguldak	B	5.7	1.6
Cartosat-1, Warsaw	B	2.5	0.6
OrbView-3, Zonguldak	A	1	1.3
IKONOS, Zonguldak	B	1.0	0.7
QuickBird, Zonguldak	B	0.61	0.8

Several high and very high resolution images have been oriented by Jacobsen (2007c). All orientations listed in Table 1 are based on geometric reconstruction or bias corrected RPC solutions. Under usual conditions, sub-pixel accuracy has been reached. In the case of KOMPSAT-1 and IRS-1C,

Zonguldak, the achieved accuracy was limited by the control point quality. In the case of OrbView-3, the accuracy exceeds the GSD, but it is below the projected pixel size. No significant difference between the orientation of level 1A-type and level 1B-type scenes can be seen. Under operational conditions with well defined control points, pixel- or even sub-pixel-accuracy can be reached.

2 AIRBORNE SYSTEMS

2.1 Introduction

Airborne CCD-line scanners at first were used for classification purposes. Their images have a different exterior orientation for every CCD-line, but within each CCD-line there is a stable geometry (Fig. 8). This is still better than scanning systems based on diodes, having a different orientation for every pixel. Without additional orientation information from GPS and inertial measurement units (IMU), the geo-reference can only be estimated using a high number of control points. For this reason, polynomial models have mostly been used. Polynomial solutions cannot be called image orientation; they are only fitting the homogenous, but geometric distorted, image to reference points. Usually they are not respecting the influencing digital elevation model. Only the geometrically more precise methods are described.

For photogrammetric application, only three-line-scanners are in use such as HRSC from DLR, Leica ADS40, the former Starlabo Starimager, Wehrli 3-DAS-2 and Jenoptronic JAS 150. The basic principle was developed as DPA by Otto Hofmann at Messerschmidt, Bölkow, Blohm, Munich around 1970 (Hofmann & Navé 1982). The first practical application came with the MOMS satellite and it was also included as HRSC in the failed first German Mars-mission. After this, the German Aerospace Centre DLR modified the HRSC for aerial application. Supported by DLR, Leica developed the ADS40.

These systems are operated together with kinematic GPS and IMU. Three-line-scanners may have separate CCD-lines on one focal plane or they may have a combination of sub-cameras, each with just a line (Fig. 9). The mathematical handling is more or less the same, because a camera system has a known geometric relation to the sub-cameras. The recording interval of the IMU is short enough to guarantee by linear interpolation no loss of accuracy for the orientation determination of any individual CCD-line. But the orientation may not be accurate or reliable enough or the orientation devices may fail.
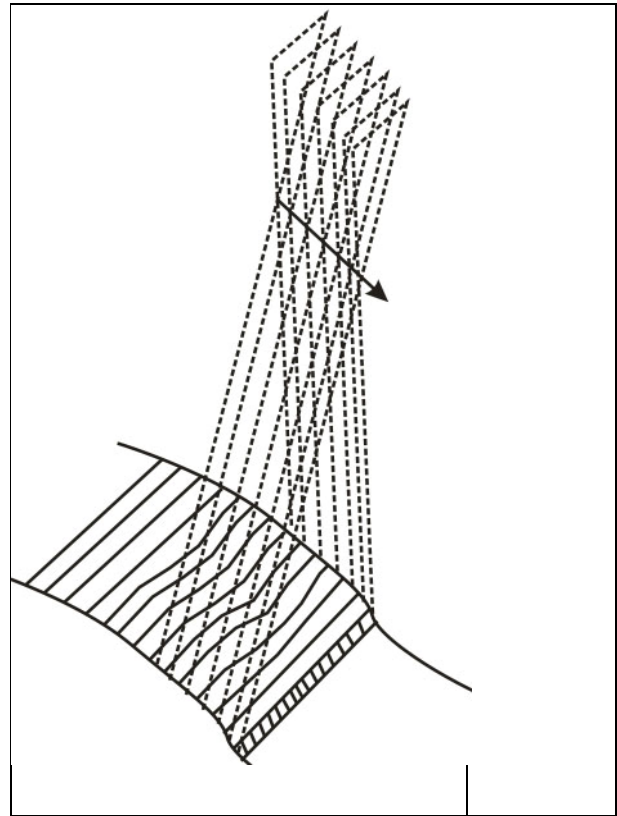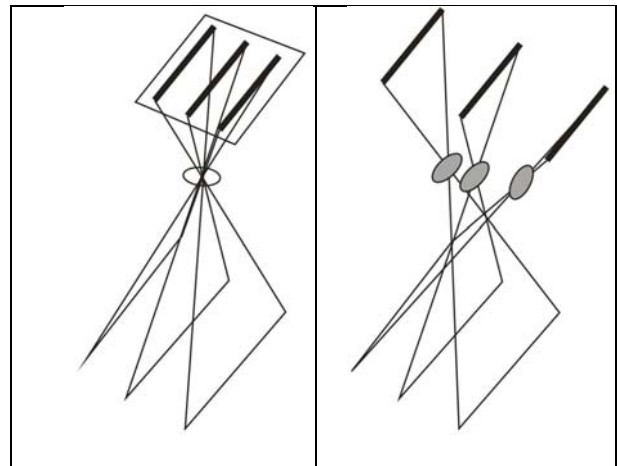

Figure 8. CCD-line image.

Figure 9. 3-line-scanner with 1 focal plane (left) and 3-line scanner with 3 optics (right).

Leica ADS40 images allow a mapping based on stereoscopic view by human operator. The direct sensor orientation is not precise enough for a stereoscopic view without disturbing y-parallaxes, and so an adjustment using tie points is required (Fricker 2001).

2.2 Aerotriangulation

With line scanner images, no classical bundle block adjustment is possible because of missing fixed connection of neighbouring lines, but the orientation is only changing continuously, so groups of CCD-lines can be joined together to "orientation images" with an orientation presented by "orientation fixes" (Hofmann & Nave 1982, Ohlhof 1995). Joining neighboured CCD-lines to orientation images,

stabilized with tie points to the images of the other view direction and supported by control points (Fig. 11), allows also approximate orientation determination of the whole system without the support of GPS and IMU. Of course, if no support by GPS and IMU is available, quite a few more control points are required. By adjustment of GPS / IMU supported three-line scanner data, only the low frequency data are improved. The high frequency data are still unchanged (Fig. 12).
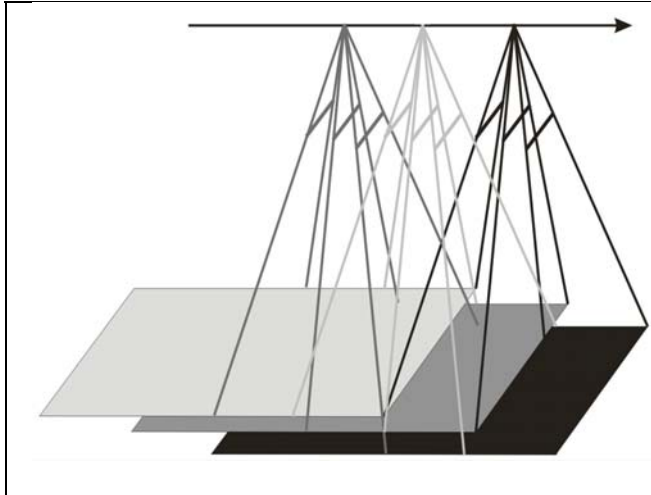

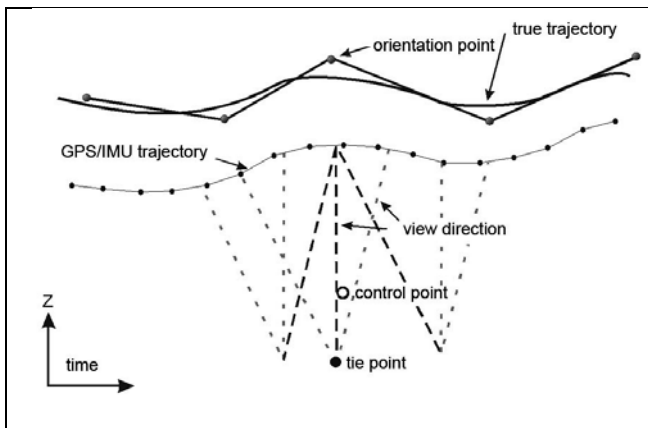Figure 10. Imaging configuration of three-line scanner.

Figure 11. Basic principle of three-line scanner block adjustment.

The aerotriangulation of the three-line sensors is possible without ground control if it is supported by GPS and IMU, but for reliability reasons and for the determination of the datum, control points are required for practical applications. Supported by control points, a standard deviation of all coordinate components is possible on the sub-pixel level (Cramer 2006). Without control points, the offsets cannot be guaranteed.
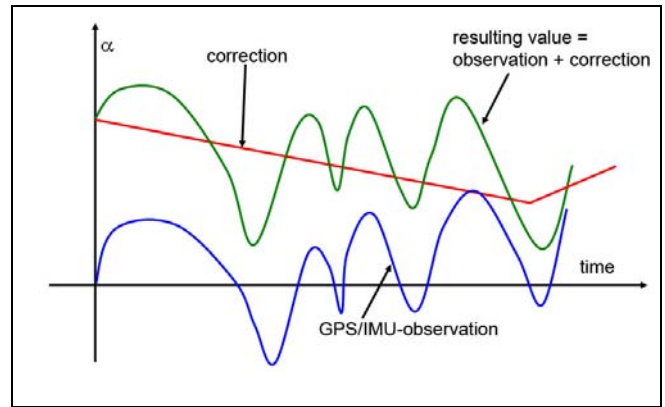

Figure 12. Correction of trajectory – high frequency observation with low frequency correction.

3 PANORAMIC IMAGERS

3.1 *Introduction*

Panoramic cameras are scanning the object from one side to the other with perspective geometry only in the line perpendicular to the scan direction (Fig. 13). They have been used in space by the US CORONA system (McDonald 1997) from 1959 up to 1972 and the Soviet/Russian KVR1000, from the air (Slama 1980) and also on the Earth (Reulke et al. 2004).
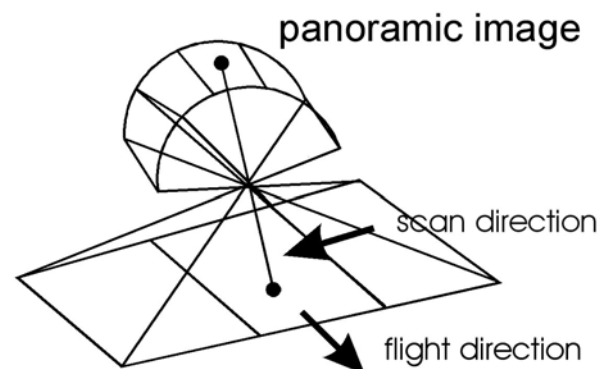
3.2 *Panoramic geometry*

Figure 13. Principle of panoramic camera.

Even if the object area is flat, the image scale is changing depending upon the relation of the focal length and the oblique distance. Across the view direction, the scale change is $1/\cos v$ with v as the nadir angle and in the view direction it is $1/\cos^2 v$. During scanning, the aircraft or satellite is moving, causing a deformation of the image geometry (Fig. 14).
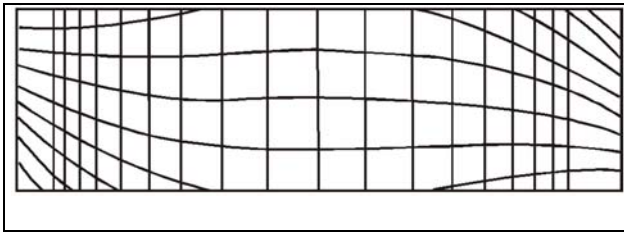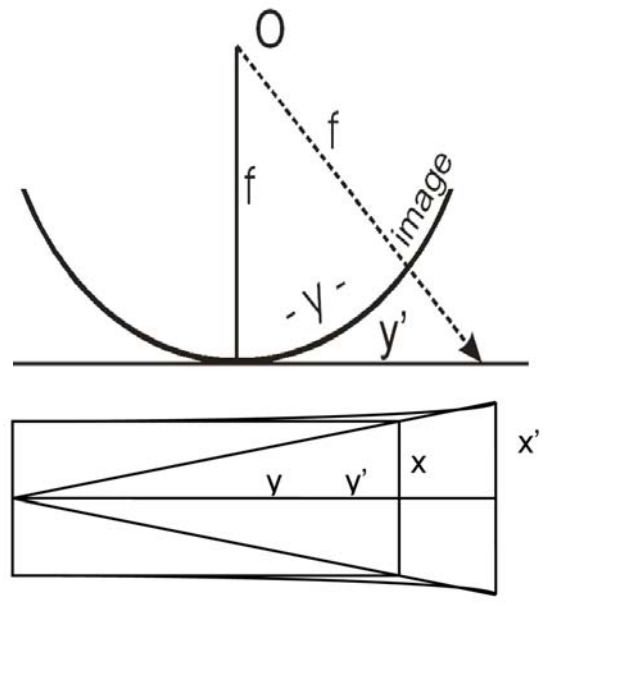
Figure 14. Panoramic image of a square grid in the object space.

Like the CCD-line images, every image line perpendicular to the scan direction has a different exterior orientation, so in aerial application the support of GPS/IMU has advantages. For the mathematical handling, the collinearity equation has to be modified for the changing scale and the changing exterior orientation. Another possibility is a correction of the panoramic image to perspective geometry without influence of the platform motion (Fig. 15).

$$y' = f \bullet \tan \frac{y}{f}$$

$$x' = \frac{x}{f} \bullet \sqrt{f^2 + y^2}$$

Figure 15. Transformation of panoramic image to perspective geometry.

$x' = x - (y/f - x/r^2) * P22$
$\qquad\qquad y' = y - (y/f - y/(f^2 + y^2)) \bullet P22$
$x' = x - \arctan y/x \bullet P23 \qquad y' = y$
$x' = x - \sin (y/300.) \bullet P24 \qquad y' = y$
$x' = x \qquad\qquad y' = y - \sin (y/300) \bullet P25$
$\quad x' = x - \sin (y/150.) \bullet P26 \qquad y' = y$

Formula 6. Special additional parameters for handling panoramic images.

The aircraft and the scanning speed is often unknown, so the influence of the platform motion has to be determined by self calibration with additional parameters in the orientation process or by bundle adjustment. In the Hannover program system BLUH, special additional parameters are available for the handling of panoramic images (Jacobsen 1988), which can be used after pre-correction to perspective geometry (Fig. 15).
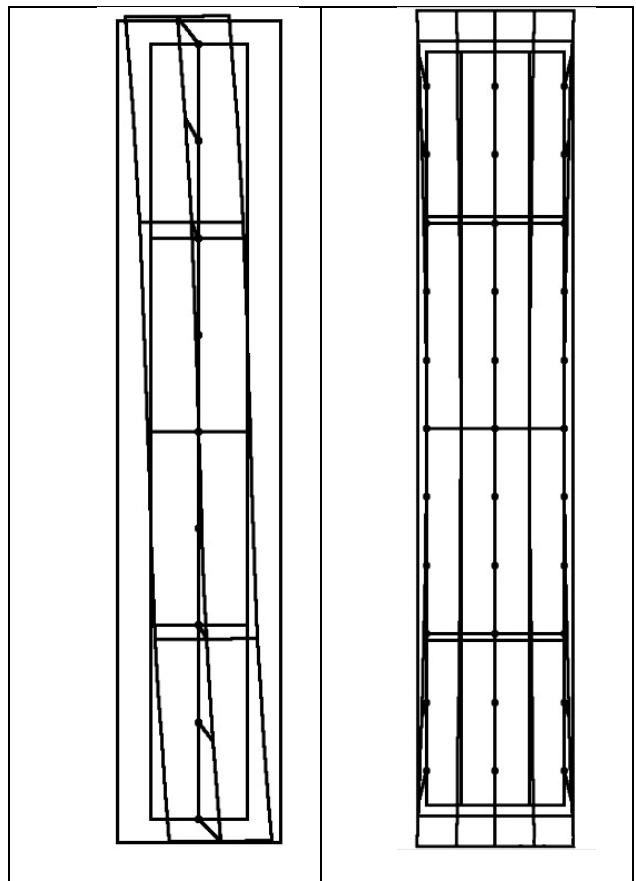
3.3 *Aerial panoramic cameras*

Figure 16. Left: dynamic effect of panoramic aerial image determined by self calibration with additional parameters. Right: effect of transformation panoramic image to perspective geometry.
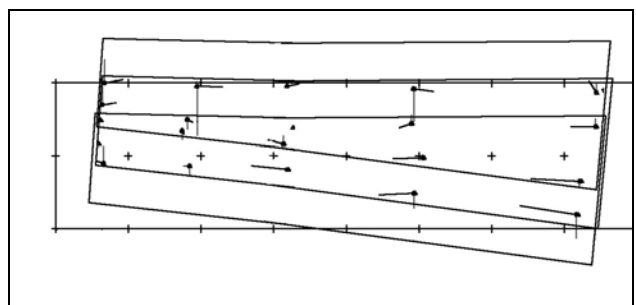

Figure 17. Block of 3 panoramic images (from centre of image – left, up to end – right).

In the example of the block adjustment of aerial panoramic images, shown in Figure 17, the scale in the image centre is 1:10,000, at the border with a nadir angle of 49° it is 1:15,300 across the view direction and 1:23,600 in the view direction. In the centre, the base to height relation is 1:12 while it is 1:18.4 at the border. Object points determined in a perspective aerial model have a homogenous accuracy in X and Y and the vertical accuracy is approximately the horizontal accuracy multiplied by the height to base relation; this is not the case for panoramic models. In panoramic image models with a nadir angle of 45°, the horizontal accuracy in the scan direction is the same as the vertical accuracy. With larger nadir angles, the vertical accuracy is better than the accuracy in the scan direction.

$$SX = \frac{hg}{f \bullet \cos \upsilon} \bullet \sigma o$$

$$SY = \sqrt{\frac{hg}{f \bullet \cos \upsilon + SZ \bullet \tan \upsilon} \bullet \sigma 0}$$

$$SZ = \frac{hg^2}{f \bullet b \bullet \cos \upsilon} \bullet \sigma o$$

Formula 7. Standard deviation of object coordinates determined by panoramic model.

Hg = flying height   f = focal length υ = nadir angle

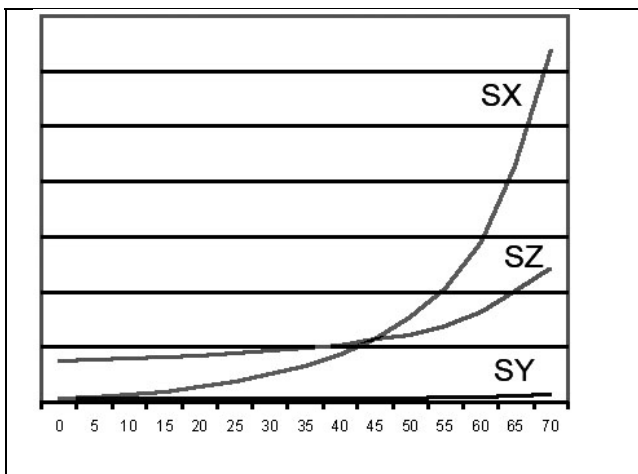σo = standard deviation of image coordinates

b = base length

Figure 18. Relative accuracy of object coordinates determined in panoramic model with base to height relation 1:12 as function of nadir angle.
horizontal = nadir angle [°]

3.4 *Spaceborne panoramic cameras*

The same handling as shown above with aerial panoramic images is possible with satellite panoramic images, but the conditions are better than in aerial images. With +/-34.5°, the largest nadir angle for a CORONA KH4B image is smaller than for aerial systems and the sensor movement is much better known than for aerial systems.
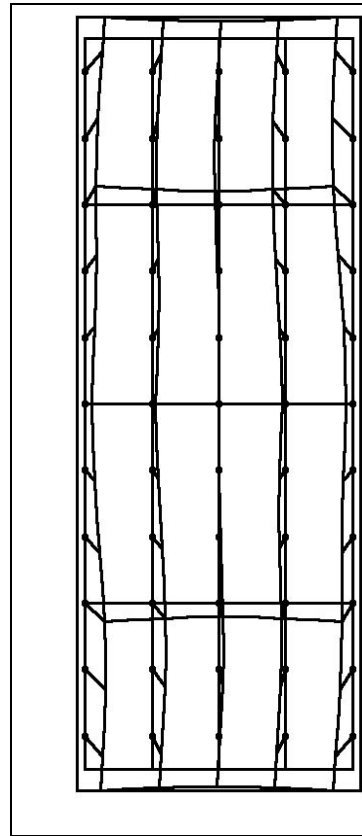

Figure 18. Systematic image errors of a CORONA stereo pair. Largest vector = 440 µm.

The most often used CORONA camera is the KH4B having a focal length of 627 mm and a film size of 55.37 mm x 756.92 mm. For this format, the difference from perspective geometry is not exceeding dx = 3.9 mm and dy = 53.4 mm, for the large image format in the y-direction. The systematic image errors (difference of mathematical model against reality), based on the additional parameters shown in Formula 6 plus affinity, for a CORONA stereo pair is shown in Figure 18. The typical S-shape caused by the sensor movement during imaging is obvious; in addition a stronger affinity can be seen. The scale difference between x and y image coordinates can be explained by the inaccurate focal length caused by the imprecise film motion during imaging. With the above mentioned handling, digital elevation models based on the convergent arranged KH4B stereo camera combination can be determined with at least a relative vertical accuracy of up to 5 m (Schneider et al. 2001).

The orientation of the Soviet / Russian KFA1000 is similar to the handling of CORONA images, with the difference that the KVR1000 was not used in a stereo combination. Instead, the Soviet Union used the combination of the panoramic KVR1000 together with perspective stereo models of the TK350.

3.5 *Terrestrial panoramic cameras*

The mathematical handling of terrestrial panoramic cameras is much simpler. The camera axis is not moving during imaging. In the vertical direction, perspective geometry exists, while in the horizontal scan direction the viewing angle is a linear function of the time, corresponding to the image coordinate component (Reulke et al. 2004). For precise point determination such terrestrial panoramic cameras need a satisfactory calibration, which is also possible by self calibration with additional parameters.

4 CONCLUSION

Today existing high resolution space imagery is competing with aerial photographs requiring similar orientation accuracy. Only with geometric correct orientation methods like geometric reconstruction and sensor oriented, bias corrected rational polynomial coefficients is this guaranteed. The approximate image orientation models like the 3-D affine transformation, direct linear transformation and terrain dependent RPCs require more and three-dimensional, well distributed control points; in addition they cannot guarantee the accuracy in any case.

Today aerial CCD-line scanner systems are in use as three-line scanners, usually supported by GPS and inertial measurement units (IMU). Based on GPS and IMU in theory no adjustment and no control points are required, but aerial triangulation solves the datum problem, guarantees the reliability and reduces disturbing y-parallaxes in the stereo models.

Panoramic images can be transformed into perspective geometry and the effect of the sensor motion during exposure can be handled by self calibration with special additional parameters. Also terrestrial panoramic imagers are in use; because of the fixed positioning during orientation, the geometric model is simple, and the system calibration may be improved by self calibration.

REFERENCES

Cramer, M. 2006. The ADS40 Vaihingen/Enz geometric performance test. *IJPRS* 60, 6: 363–374.

Dial, G. & Grodecki, J. 2002. IKONOS Accuracy without Ground Control, Pecora 15 / Land Satellite Information IV / ISPRS Com. I, Denver 2002. *Int. Arch. PhRS* XXXIV, part 1: 31–35.

Gervaix, F. 2002. Aerotriangulation: auch für den ADS40 Luftbildsensor? *Photogrammetrie, Fernerkundung, Geoinformation* 2002: 85–91.

Grodecki, J. 2001. IKONOS Stereo Feature Extraction – RPC Approach. *ASPRS annual conference St. Louis.*

Fricker, P. 2001. ADS40 – Progress in digital aerial data collection. *Photogrammetric Week 01*: 105–116. Heidelberg: Wichmann Verlag.

Hanley, H.B., Yamakawa, T. & Fraser, C.S. 2002. Sensor Orientation for High Resolution Imagery, Pecora 15 / Land Satellite Information IV / ISPRS Com. I, Denver. *Int. Arch. PhRS* XXXIV, part 1: 69–75.

Hofmann, O. & Navé, P. 1982. DPS – a digital photogrammetric system for producing digital elevation models and orthophotos by means of linear array scanner imagery. ISPRS Com III, Helsinki. *Int. Arch. PhRS* 24–III: 216–227.

Jacobsen, K. 1988. Handling of Panoramic and Extreme High Oblique Photographs in Analytical Plotters, ISPRS congress Kyoto 1988. *Int. Arch. PhRS* XXVII, B2: 232–237.

Jacobsen, K. 1997. Calibration of IRS–1C PAN–camera. *Joint Workshop "Sensors and Mapping from Space", Hannover 1997.* http://www.ipi.uni–hannover.de/ (Feb. 18th, 2008).

Jacobsen, K. 2007a. Digital Height Models by Cartosat–1, ISPRS Hannover Workshop 2007. *Int. Arch. PhRS* XXXVI Part I/W51.

Jacobsen, K. 2007b. Geometry of Digital Frame Cameras, *ASPRS Annual Conference, Tampa 2007.*

Jacobsen, K. 2007c. Orientation of high resolution optical space images. A*SPRS Annual Conference*, *Tampa 2007.*

McDonald, R. (ed.) 1997. *CORONA between the sun & the earth.* ASPRS. ISBN 1-57083-041-X.

Ohlhof, T. 1995. Block triangulation using three-line images. *Photogrammetric Week 1995*: 197–200. Heidelberg: Wichmann Verlag.

Passini, R. & Jacobsen, K. 2004. Accuracy Analysis of Digital Orthophotos from Very High Resolution Imagery. ISPRS Congress, Istanbul 2004. *Int. Arch. PhRS* XXXV, B4: 695–700.

Reulke, R., Wehr, A. & Griesbach, D. 2004. High resolution mapping using CCD–line camera and laser scanner with integrated position and orientation system, ISPRS congress Istanbul. *Int. Arch. PhRS* XXXV, B3: 506–511.

Schneider, T., Seitz, R., Förster, B. & Jacobsen, K. 2001. Remote Sensing Based Parameter Extraction for Erosion Control Purposes in the Loess Plateau of China. *ISPRS Workshop High Resolution Mapping from Space 2001.*

Slama, C. (ed.). 1980. *Manual of Photogrammetry*, Fourth edition, chapter 4.2.2 Panoramic Cameras: 196–207. ASPRS. ISBN 0-937294-01-2.

Toutin, Th. 2003. Error tracking in IKONOS geometric processing using a 3D parametric modeling. *Photogramm. Eng. Remote Sens.* 69, 1: 43–51.